

# MINIMUM DRAG SHAPE IN TWO-DIMENSIONAL VISCOUS FLOW

DO WAN KIM

*Department of Mathematics, Korea Advanced Institute of Science and Technology, Yusong-gu, Taejon 305-701, South Korea*

AND

MOON-UHN KIM

*Department of Mechanical Engineering, Korea Advanced Institute of Science and Technology, Yusong-gu, Taejon 305-701, South Korea*

## SUMMARY

The problem of finding the shape of a body with smallest drag in a flow governed by the two-dimensional steady Navier–Stokes equations is considered. The flow is expressed in terms of a streamfunction which satisfies a fourth-order partial differential equation with the biharmonic operator as principal part. Using the adjoint variable approach, both the first- and second-order necessary conditions for the shape with smallest drag are obtained. An algorithm for the calculation of the optimal shape is proposed in which the first variations of solutions of the direct and adjoint problems are incorporated. Numerical examples show that the algorithm can produce the optimal shape successfully.

KEY WORDS: smallest drag; first-order necessary condition; second-order necessary condition

## 1. INTRODUCTION

This paper considers the minimum drag profile in two-dimensional steady incompressible viscous flow. Particular emphasis is laid on providing an efficient algorithm for the computation of optimal shapes. Although much literature is available on the domain optimization problem of continuum structural systems,<sup>1</sup> only a few studies on shape optimization problems in viscous flow have been reported. Pironneau has obtained the first-order necessary conditions for optimal profiles in Stokes flow<sup>2</sup> and Navier–Stokes flow.<sup>3</sup> Mironov<sup>4</sup> has obtained the necessary conditions for minimum drag of a body when the flow is described by the steady Navier–Stokes equations. An algorithm for finding the optimal shape has been proposed, though programming was not attempted.<sup>2</sup> Later Glowinski and Pironneau<sup>5</sup> determined numerically the approximate shape of a given area with smallest drag in laminar flow using the boundary layer approximation. Recently Çabuk and Modi<sup>6</sup> derived the first-order necessary condition for the optimal profile of a plane diffuser providing the maximum static pressure rise and performed numerical computations.

In the present study the first- and second-order necessary conditions for the optimal profile minimizing the rate of energy dissipation in steady two-dimensional viscous flow are derived. The flow field is expressed in terms of a streamfunction which satisfies a non-linear fourth-order partial differential equation with the biharmonic operator as principal part. In order to calculate the variations of the objective functional, we derive the boundary value problems satisfied by the first and second

variations of the solution in a formal way using the boundary perturbation method.<sup>7</sup> Mathematical justification of the characterization of variations of the solution is provided under some regularity assumptions. (Appendix I). Having found the first and second variations of the solution, the first- and second-order necessary conditions of Kuhn–Tucker type for optimality are obtained with the aid of an appropriate adjoint system. The approach in the appendices is a direct generalization of that developed by Fujii, who treated the domain optimization problem constrained by either a Dirichlet<sup>8,9</sup> or a Neumann<sup>10</sup> boundary value problem of a second-order differential equation with the harmonic operator as principal part.

Based on the first- and second-order necessary optimality conditions, a numerical algorithm is proposed in which the first variation of the solution is incorporated. Solutions of the Navier–Stokes equations, the first variation and the adjoint problem are computed using the finite difference method. If a profile sufficiently close to the optimal shape can be assumed, the proposed algorithm is found to yield the optimal profile within a few iterations.

## 2. PROBLEM STATEMENT

We consider the steady two-dimensional incompressible viscous flow in a multiply connected domain  $\Omega$  bounded internally by the surface of a body  $\Gamma^b$  at rest and externally by a surface  $\Gamma^e$  on which the velocity field  $\mathbf{V} = (V_1, V_2)$  is specified (Figure 1). For two-dimensional incompressible flow it is convenient to introduce the streamfunction  $u$  such that

$$\frac{\partial u}{\partial y} = v_1, \quad \frac{\partial u}{\partial x} = -v_2.$$

where  $\mathbf{v} = (v_1, v_2)$  denotes the velocity field. The governing equation and the boundary conditions are written in terms of the streamfunction as

$$\begin{aligned} Re^{-1} \Delta^2 u &= \frac{\partial(\Delta u, u)}{\partial(x, y)} \quad \text{on } \Omega, \\ u|_{\Gamma^b} &= 0, \quad \frac{\partial u}{\partial n}|_{\Gamma^b} = 0, \quad \frac{\partial u}{\partial x}|_{\Gamma^e} = -V_2, \quad \frac{\partial u}{\partial y}|_{\Gamma^e} = V_1. \end{aligned} \quad (1)$$

In the above, all the quantities are non-dimensionalized and  $Re$  denotes the Reynolds number.

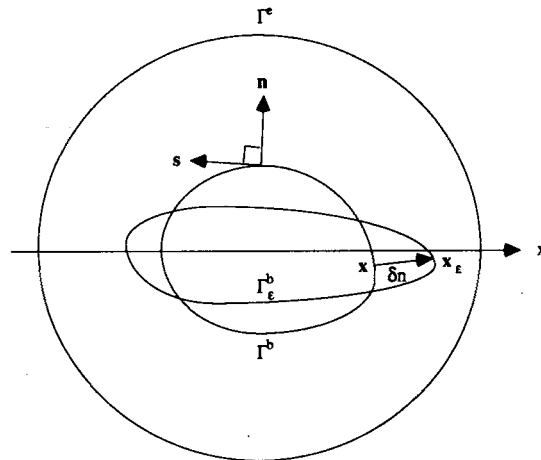


Figure 1. Laminar flow over a body profile.  $\Gamma^b_\epsilon$  is the modified profile of  $\Gamma^b$  due to a boundary perturbation  $\delta n$ . The outer boundary  $\Gamma^e$  remains unchanged

Let us consider the following domain optimization problem.

*Problem*

Find the domain which minimizes

$$J(\Omega, u) = \int_{\Omega} [(u_{yy} - u_{xx})^2 + 4u_{xy}^2] d\Omega \equiv \int_{\Omega} g d\Omega \quad (2)$$

with respect to  $\Gamma^b$  subject to the isoperimetric constraint

$$I(\Omega) = \int_{\Omega} d\Omega = \text{const.} \quad (3)$$

The functional  $J$  defined by (2) is proportional to the rate of energy dissipation. Here  $u$  is the solution of boundary value problem (1) and it is assumed that the velocity distribution on the surface  $\Gamma^e$  does not depend on the shape of the body  $\Gamma^b$ . In the present study, uniform flow ( $\mathbf{V} = \text{const.}$ ) far from the body  $\Gamma^b$  is considered and  $|\mathbf{V}|$  is taken as the characteristic velocity. It should be noted that if the flow on the surface  $\Gamma^e$  is uniform, then the drag coefficient on  $\Gamma^b$  approaches  $J/Re$  as the minimum distance from the body surface  $\Gamma^b$  to the surface  $\Gamma^e$  tends to infinity and thus the present problem of the minimum energy dissipation rate becomes equivalent to the minimum drag problem.

### 3. MATHEMATICAL PRELIMINARIES

In this section, expressions of the first and second variations of the objective functional with respect to the variation of the body surface, which is assumed to be sufficiently smooth, are derived using the first and second variations of the solution of boundary value problem (1).

Firstly let us define the boundary variation. Let  $\rho(s)$  and  $\sigma(s)$  be arbitrary smooth functions of arc length defined on  $\Gamma^b$  and let  $\varepsilon$  be a positive number. Let each point on  $\Gamma^b$  be moved by  $\delta n$  along the outward normal direction. The boundary variation  $\delta n$  is given by  $\delta n = \varepsilon\rho(s) + \varepsilon^2\sigma(s)$ . The curve constructed in this way is denoted by  $\Gamma_{\varepsilon}^b$ , which is smooth for sufficiently small  $\varepsilon$  (Figure 1). Since we are interested in the optimal shape of the body, the exterior boundary  $\Gamma^e$  is kept unchanged. Let  $\Omega_{\varepsilon}$  denote the domain enclosed by  $\Gamma^e$  and  $\Gamma_{\varepsilon}^b$  and let  $u_{\varepsilon}$  be the solution of (1) in the new domain  $\Omega_{\varepsilon}$ .

Throughout the present work we assume the following.

- A1. The classical solutions  $u$  and  $u_{\varepsilon}$  exist and are unique.
- A2. There exist sufficiently smooth functions  $\phi$  and  $\psi$  defined on  $\bar{\Omega}$  such that

$$u_{\varepsilon}(\mathbf{x}) - u(\mathbf{x}) = \varepsilon\phi(\mathbf{x}) + \varepsilon^2\psi(\mathbf{x}) + O(\varepsilon^2), \quad \mathbf{x} \in \Omega \cap \Omega_{\varepsilon},$$

$$D^{\alpha}u_{\varepsilon} - D^{\alpha}u = \varepsilon D^{\alpha}\phi + \varepsilon^2 D^{\alpha}\psi + O(\varepsilon^3),$$

$$D^{\alpha} = \partial^{|\alpha|} / \partial x^{\alpha_i} \partial y^{\alpha_j}, \quad |\alpha| = \alpha_i + \alpha_j, \quad \alpha_i \geq 0, \quad \alpha_j \geq 0, \quad |\alpha| \leq 4.$$

We call  $\phi$  and  $\psi$  the first and second variations of the solution respectively.

Since both  $u_{\varepsilon}$  and  $u$  satisfy (1), it can be easily shown that the first and second variations  $\phi$  and  $\psi$  satisfy the equations

$$Re^{-1}\Delta^2\phi = \frac{\partial(\Delta u, \phi)}{\partial(x, y)} + \frac{\partial(\Delta\phi, u)}{\partial(x, y)} \quad \text{in } \Omega \cap \Omega_{\varepsilon}, \quad (4a)$$

$$Re^{-1}\Delta^2\psi = \frac{\partial(\Delta\phi, \phi)}{\partial(x, y)} + \frac{\partial(\Delta u, \psi)}{\partial(x, y)} + \frac{\partial(\Delta\psi, u)}{\partial(x, y)} \quad \text{in } \Omega \cap \Omega_{\varepsilon}. \quad (4b)$$

Next let us derive the conditions satisfied by  $\phi$  and  $\psi$  on  $\Gamma^b$ . Consider a point  $\mathbf{x}$  on  $\Gamma^b$  and a corresponding point  $\mathbf{x}_\varepsilon$  on  $\Gamma_\varepsilon^b$  such that  $\mathbf{x}_\varepsilon$  lies on the outward normal  $\mathbf{n}$  (Figure 1). Assume that the boundary variation  $\delta n = \varepsilon\rho + \varepsilon^2\sigma$  is positive.

Taylor expansion of  $u_\varepsilon(\mathbf{x}_\varepsilon)$  and  $(\partial u_\varepsilon/\partial n_\varepsilon)(\mathbf{x}_\varepsilon)$  about the point  $\mathbf{x}$  along the normal direction  $\mathbf{n}$  are shown to be

$$\begin{aligned} u_\varepsilon(\mathbf{x}_\varepsilon) &= u + \varepsilon \left( \phi + \rho \frac{\partial u}{\partial n} \right) + \varepsilon^2 \left( \psi + \rho \frac{\partial \phi}{\partial n} + \sigma \frac{\partial u}{\partial n} + \frac{1}{2} \rho^2 \frac{\partial^2 u}{\partial n^2} \right) + O(\varepsilon^3), \\ \frac{\partial u_\varepsilon}{\partial n_\varepsilon}(\mathbf{x}_\varepsilon) &= \frac{\partial u}{\partial n} + \varepsilon \left( \frac{\partial \phi}{\partial n} + \rho \frac{\partial^2 u}{\partial n^2} \right) + \varepsilon^2 \left\{ \frac{\partial \psi}{\partial n} + \rho \left( \frac{\partial^2 \phi}{\partial n^2} + \kappa \frac{\partial \phi}{\partial n} \right) + \sigma \frac{\partial^2 u}{\partial n^2} \right. \\ &\quad \left. + \rho^2 \left[ \frac{1}{2} \left( n_1 \frac{\partial^2 u_x}{\partial n^2} + n_2 \frac{\partial^2 u_y}{\partial n^2} \right) + \kappa \frac{\partial^2 u}{\partial n^2} \right] \right. \\ &\quad \left. + \frac{\partial \rho}{\partial s} \left[ n_2 \phi_x - n_1 \phi_y + \rho \left( n_2 \frac{\partial u_x}{\partial n} - n_1 \frac{\partial u_y}{\partial n} \right) \right] \right\} + O(\varepsilon^3), \end{aligned}$$

where  $\mathbf{n} = (n_1, n_2)$  and  $\kappa$  denotes the curvature. On the right-hand sides of the above equations the dependence on the point  $\mathbf{x}$  has been omitted for brevity. In obtaining the expression for  $\partial u_\varepsilon/\partial n_\varepsilon$ , we have used

$$\mathbf{n}_\varepsilon = \mathbf{n} + \varepsilon \left( \kappa \rho \mathbf{n} - \frac{\partial \rho}{\partial s} \mathbf{s} \right) + \varepsilon^2 \left( \kappa \sigma \mathbf{n} - \frac{\partial \sigma}{\partial s} \mathbf{s} \right) + O(\varepsilon^3),$$

where  $\mathbf{s}$  denotes the unit tangent vector at  $\mathbf{x} \in \Gamma^b$ . Noting that

$$\frac{\partial f_x}{\partial n} = n_1 \frac{\partial^2 f}{\partial n^2} - n_2 \left[ \frac{\partial}{\partial s} \left( \frac{\partial f}{\partial n} \right) + \kappa \frac{\partial f}{\partial s} \right] \quad \text{and} \quad \frac{\partial f_y}{\partial n} = n_2 \frac{\partial^2 f}{\partial n^2} + n_1 \left[ \frac{\partial}{\partial s} \left( \frac{\partial f}{\partial n} \right) + \kappa \frac{\partial f}{\partial s} \right]$$

for any  $f \in C^2$ , we have

$$n_1 \frac{\partial^2 u_x}{\partial n^2} + n_2 \frac{\partial^2 u_y}{\partial n^2} = \frac{\partial(\Delta u)}{\partial n} - \kappa \frac{\partial^2 u}{\partial n^2}.$$

The no-slip condition on  $\Gamma^b$  requires that

$$\phi = 0, \quad \frac{\partial \phi}{\partial n} = -\rho \frac{\partial^2 u}{\partial n^2}, \quad (5a)$$

$$\psi = -\frac{1}{2} \rho \frac{\partial \phi}{\partial n}, \quad \frac{\partial \psi}{\partial n} = \frac{1}{2} \kappa \rho^2 \frac{\partial^2 u}{\partial n^2} - \sigma \frac{\partial^2 u}{\partial n^2} - \frac{1}{2} \rho^2 \frac{\partial(\Delta u)}{\partial n} - \rho \frac{\partial^2 \phi}{\partial n^2}, \quad (5b)$$

since  $u = \partial u/\partial n = 0$  on  $\Gamma^b$ . On the fixed external boundary  $\Gamma^e$ ,

$$\phi = \frac{\partial \phi}{\partial n} = 0, \quad (5a')$$

$$\psi = \frac{\partial \psi}{\partial n} = 0, \quad (5b')$$

since  $u$  and  $u_\varepsilon$  satisfy the same boundary conditions.

The above derivation of the first and second variations of the solution  $u$  with respect to the boundary variation  $\delta n$  is purely formal. However, in Appendix I we provide the mathematical justification of the characterization of the two variations of the solution under some regularity assumptions by extending the approach of Fujii.<sup>8-10</sup> The second variation of the solution enables us to obtain the second-order necessary conditions for an optimal domain.

The first and second variations of the functional  $J$ , namely  $\delta J^{(1)}$  and  $\delta J^{(2)}$ , are defined by

$$J(\Omega_\varepsilon, u_\varepsilon) - J(\Omega, u) = \varepsilon \delta J^{(1)} + \varepsilon^2 \delta J^{(2)} + O(\varepsilon^3)$$

and are expressed as

$$\delta J^{(1)} = \int_{\Gamma^b} g \rho \, d\Gamma + 2 \int_{\Omega} [(u_{yy} - u_{xx})(\phi_{yy} - \phi_{xx}) + 4u_{xy}\phi_{xy}] \, d\Omega, \quad (6)$$

$$\begin{aligned} \delta J^{(2)} = & \int_{\Gamma^b} g \sigma \, d\Gamma + 2 \int_{\Gamma^b} \rho [(u_{yy} - u_{xx})(\phi_{yy} - \phi_{xx}) + 4u_{xy}\phi_{xy}] \, d\Gamma \\ & + 2 \int_{\Omega} [(u_{yy} - u_{xx})(\psi_{yy} - \psi_{xx}) + 4u_{xy}\psi_{xy}] \, d\Omega \\ & + \frac{1}{2} \int_{\Gamma^b} \left( \kappa g + \frac{\partial g}{\partial n} \right) \rho^2 \, d\Gamma + \int_{\Omega} [(\phi_{yy} - \phi_{xx})^2 + 4\phi_{xy}] \, d\Omega, \end{aligned} \quad (7)$$

where  $g$  is the integrand of the dissipation energy functional  $J$ :

$$g = (u_{yy} - u_{xx})^2 + 4u_{xy}^2.$$

By introducing an adjoint variable  $p$  as the solution of the boundary value problem

$$\begin{aligned} Re^{-1} \Delta^2 p + \Delta \frac{\partial(p, u)}{\partial(x, y)} - \frac{\partial(p, \Delta u)}{\partial(x, y)} &= - \frac{\partial(\Delta u, u)}{\partial(x, y)} \quad \text{in } \Omega, \\ p|_{\Gamma^b} &= 0, \quad \frac{\partial p}{\partial n}|_{\Gamma^b} = 0, \quad p|_{\Gamma^c} = \frac{\partial p}{\partial n}|_{\Gamma^c} = 0, \end{aligned} \quad (8)$$

expression (6) for the first variation  $\delta J^{(1)}$  can be rewritten as

$$\delta J^{(1)} = - \int_{\Gamma^b} \left[ \left( \frac{\partial^2 u}{\partial n^2} \right)^2 + 2 \frac{\partial^2 p}{\partial n^2} \frac{\partial^2 u}{\partial n^2} \right] \rho \, d\Gamma. \quad (9)$$

The proof is given in Appendix II.

With the help of the following equality, which has been obtained by expressing the integrands in  $(n, s)$ -co-ordinates and considering the boundary conditions,

$$\begin{aligned} & 2 \int_{\Gamma^b} \rho [(u_{yy} - u_{xx})(\phi_{yy} - \phi_{xx}) + 4u_{xy}\phi_{xy}] \, d\Gamma + \frac{1}{2} \int_{\Gamma^b} \left( \kappa g + \frac{\partial g}{\partial n} \right) \rho^2 \, d\Gamma \\ &= \int_{\Gamma^b} \left[ 2\rho \frac{\partial^2 u}{\partial n^2} \frac{\partial^2 \phi}{\partial n^2} + \rho^2 \frac{\partial^2 u}{\partial n^2} \frac{\partial(\Delta u)}{\partial n} + \frac{1}{2} \kappa \rho^2 \left( \frac{\partial^2 u}{\partial n^2} \right)^2 \right] \, d\Gamma, \end{aligned}$$

the second variatioin  $\delta J^{(2)}$  can be rewritten in the form

$$\begin{aligned} \delta J^{(2)} = & \int_{\Gamma^b} \frac{\partial^2 u}{\partial n^2} \left( -\sigma \frac{\partial^2 u}{\partial n^2} + \frac{3}{2} \kappa \rho^2 \frac{\partial^2 u}{\partial n^2} - \rho^2 \frac{\partial(\Delta u)}{\partial n} - \rho^2 \frac{\partial(\Delta p)}{\partial n} \right) d\Gamma \\ & - 2 \int_{\Gamma^b} \frac{\partial^2 p}{\partial n^2} \left( \sigma \frac{\partial^2 u}{\partial n^2} - \frac{1}{2} \kappa \rho^2 \frac{\partial^2 u}{\partial n^2} + \frac{1}{2} \rho^2 \frac{\partial(\Delta u)}{\partial n} \right) d\Gamma \\ & + \int_{\Omega} [(\phi_{yy} - \phi_{xx})^2 + 4\phi_{xy}^2] d\Omega + 2Re \int_{\Omega} \Delta \phi \frac{\partial(p, \phi)}{\partial(x, y)} d\Omega. \end{aligned} \quad (10)$$

The isoperimetric constraint (3) requires that  $\rho$  and  $\sigma$  should satisfy

$$\int_{\Gamma^b} \rho d\Gamma = 0, \quad (11)$$

$$\int_{\Gamma^b} (\sigma + \frac{1}{2} \kappa \rho^2) d\Gamma = 0. \quad (12)$$

If  $\Omega$  is an optimal domain, then  $\delta J^{(1)} = 0$  holds for every  $\rho$  that satisfies constraint (11). Thus, by the well-known Lagrange multiplier rule, there exists a constant  $\lambda$  (Lagrange multiplier) such that

$$-\left(\frac{\partial^2 u}{\partial n^2}\right)^2 - 2 \frac{\partial^2 p}{\partial n^2} \frac{\partial^2 u}{\partial n^2} = \lambda \quad \text{on } \Gamma^b. \quad (13)$$

Furthermore, since  $\Omega$  attains the minimum of  $J$ , the second variation  $\delta J^{(2)}$  must satisfy the inequality

$$\delta J^{(2)} \geq 0$$

for any  $\rho$  and  $\sigma$  satisfying (11) and (12). The second-order necessary condition for optimality can be written as

$$\begin{aligned} & \int_{\Gamma^b} \rho^2 \frac{\partial^2 u}{\partial n^2} \left( \kappa \frac{\partial^2 u}{\partial n^2} - \frac{\partial(\Delta u)}{\partial n} - \frac{\partial(\Delta p)}{\partial n} - \frac{\partial^2 p}{\partial n^2} \frac{\partial(\Delta u)}{\partial n} \right) d\Gamma \\ & + \int_{\Omega} [(\phi_{yy} - \phi_{xx})^2 + 4\phi_{xy}^2] d\Omega + 2Re \int_{\Omega} \Delta \phi \frac{\partial(p, \phi)}{\partial(x, y)} d\Omega - \lambda \int_{\Gamma^b} \kappa \rho^2 d\Gamma \geq 0 \end{aligned} \quad (14)$$

for any  $\rho$  which satisfies constraint (11). In (14) the second-order boundary variation  $\sigma$  has been eliminated by using relation (12). It is noteworthy that the above second-order necessary condition is expressed in terms of solutions of the direct and adjoint problems and the first variation.

We note that the first-order necessary condition (13) is equivalent to that derived by Pironneau.<sup>3</sup> Setting  $\mathbf{v} = (v_1, v_2) = (\partial u / \partial y, -\partial u / \partial x)$  and  $\mathbf{w} = (w_1, w_2) = (\partial p / \partial y, -\partial p / \partial x)$  and taking the curl of (3.2) in Reference 3, we obtain equation (8) for the adjoint variable  $p$ . Furthermore, the no-slip condition  $\mathbf{v} = 0$  on  $\Gamma^b$  yields

$$\left\| \frac{\partial \mathbf{v}}{\partial n} \right\|^2 + 2 \frac{\partial \mathbf{w}}{\partial n} \cdot \frac{\partial \mathbf{v}}{\partial n} = \left( \frac{\partial^2 u}{\partial n^2} \right)^2 + 2 \frac{\partial^2 p}{\partial n^2} \frac{\partial^2 u}{\partial n^2} \quad \text{on } \Gamma^b.$$

#### 4. NUMERICAL ANALYSIS

For searching the optimal shape, it is crucial to provide an efficient profile modification process. One difficulty in the iterative process is finding a new profile which satisfies the optimality condition (13)

most closely in spite of the fact that the solution for the new profile is not known *a priori*. In the present study we propose an algorithm in which the first variations of solutions of the direct and adjoint problems are incorporated. In the numerical experiment the optimum body is assumed to be symmetric with respect to the outer uniform flow direction.

#### 4.1. Profile modification method

In this subsection we propose an iterative profile modification method whereby a new profile satisfying the optimality condition (13) as closely as possible is constructed from a given shape. Firstly we denote the first variation  $\pi$  of the solution  $p$  of adjoint problem (8) corresponding to the boundary variation  $\varepsilon\rho(s)$ . Let  $p_\varepsilon$  be the solution of (8) in the new domain  $\Omega_\varepsilon$ ; then we have

$$p_\varepsilon(\mathbf{x}) - p(\mathbf{x}) = \varepsilon\pi(\mathbf{x}) + O(\varepsilon^2) \quad \text{for any } \mathbf{x} \in \Omega \cap \Omega_\varepsilon.$$

We can derive the governing equation for  $\pi$  by the same procedure as for  $\phi$ :

$$\begin{aligned} Re^{-1}\Delta^2\pi + \Delta\left(\frac{\partial(\pi, u)}{\partial(x, y)} + \frac{\partial(p, \phi)}{\partial(x, y)}\right) - \frac{\partial(\pi, \Delta u)}{\partial(x, y)} &= \frac{\partial(p, \Delta\phi)}{\partial(x, y)} - \frac{\partial(\Delta\phi, u)}{\partial(x, y)} - \frac{\partial(\Delta u, \phi)}{\partial(x, y)} \quad \text{in } \Omega, \\ \pi|_{\Gamma^b} &= 0, \quad \frac{\partial\pi}{\partial n}\Big|_{\Gamma^b} = -\rho \frac{\partial^2 p}{\partial n^2}, \quad \pi|_{\Gamma^e} = \frac{\partial\pi}{\partial n}\Big|_{\Gamma^e} = 0. \end{aligned} \quad (15)$$

It should be noted that the first variations  $\phi$  and  $\pi$  are linear in  $\rho$ . Let  $\phi_i$  and  $\pi_i$  be the first variations corresponding to the boundary variation  $\rho_i$ . Then, corresponding to the boundary variation

$$\rho = \sum_{i=1}^N a_i \rho_i, \quad (16)$$

the first variations  $\phi$  and  $\pi$  are given by

$$\phi = \sum_{i=1}^N a_i \phi_i, \quad \pi = \sum_{i=1}^N a_i \pi_i. \quad (17a, b)$$

Let  $\Gamma_\varepsilon$  be the body profile modified from an initially chosen profile  $\Gamma_0$  by a boundary variation  $\varepsilon\rho(s)$  and let

$$\Lambda_\varepsilon = \left(\frac{\partial^2 u_\varepsilon}{\partial n^2}\right)^2 + 2\left(\frac{\partial^2 u_\varepsilon}{\partial n^2}\right)\left(\frac{\partial^2 p_\varepsilon}{\partial n^2}\right) \quad \text{on } \Gamma_\varepsilon. \quad (18)$$

Then it is desirable to select  $\Gamma_\varepsilon$  (or  $\varepsilon\rho$ ) on which the optimality condition (13), the constancy of  $\Lambda_\varepsilon$ , is satisfied as closely as possible. Since  $u_\varepsilon$  and  $p_\varepsilon$  can be approximated by

$$u_\varepsilon = u_0 + \varepsilon\phi, \quad p_\varepsilon = p_0 + \varepsilon\pi,$$

$\Lambda_\varepsilon$  is approximately written as

$$\begin{aligned} \Lambda_\varepsilon &= \left(\frac{\partial^2 u_0}{\partial n^2}\right)^2 + 2\left(\frac{\partial^2 u_0}{\partial n^2}\right)\left(\frac{\partial^2 p_0}{\partial n^2}\right) + 2\varepsilon\left[\frac{\partial^2 u_0}{\partial n^2}\left(\frac{\partial^2 \phi}{\partial n^2} + \frac{\partial^2 \pi}{\partial n^2}\right) + \frac{\partial^2 p_0}{\partial n^2} \frac{\partial^2 \phi}{\partial n^2}\right] + O(\varepsilon^2) \\ &\equiv \Lambda_0 + \varepsilon\delta\Lambda_0 + O(\varepsilon^2) \quad \text{on } \Gamma_\varepsilon. \end{aligned}$$

Although  $\Lambda_\varepsilon$  is defined on  $\Gamma_\varepsilon$ , it can be evaluated approximately in terms of  $u_0, p_0, \phi, \pi$  and  $\rho$  on the initially chosen  $\Gamma_0$ :

$$\Lambda_\varepsilon = \Lambda_0(\xi) + \varepsilon\left(\frac{\partial\Lambda_0(\xi)}{\partial n}\rho(\xi) + \delta\Lambda_0(\xi)\right) + O(\varepsilon^2), \quad \xi \in \Gamma_0. \quad (19)$$

Upon applying expressions (16) and (17a, b) to (19), the unknown constant  $a_k$  are determined by requiring that the difference between  $\Lambda_\varepsilon$  given by (19) and a constant denoted by  $\lambda_0$  (not yet determined) becomes least in the mean square sense. That is, we seek constants  $\lambda_0$  and  $a_k$  ( $k = 1, \dots, N$ ) which minimize the functional

$$C(\lambda_0; \alpha_1, \dots, \alpha_N) = \int_{\Gamma_0} \left\{ \Lambda_0 + \sum_{j=1}^N \alpha_j \left[ \rho_j \frac{\partial \Lambda_0}{\partial n} + 2 \frac{\partial^2 u_0}{\partial n^2} \left( \frac{\partial^2 \phi_j}{\partial n^2} + \frac{\partial^2 \pi_j}{\partial n^2} \right) + 2 \frac{\partial^2 p_0}{\partial n^2} \frac{\partial^2 \phi_j}{\partial n^2} \right] - \lambda_0 \right\}^2 d\Gamma, \quad (20)$$

where  $\alpha_k = \varepsilon a_k$ . Since the approximate expression (19) for  $\Lambda_\varepsilon$  becomes inaccurate for large  $\varepsilon$ , we impose the following constraint to ensure that the variation is not too large:

$$\alpha_1^2 + \dots + \alpha_N^2 \leq \varepsilon_0^2, \quad (21)$$

where  $\varepsilon_0$  is a small constant given beforehand.

#### 4.2. Proposed algorithm

Based on the discussion in the previous section, we propose an algorithm for finding the minimum drag profile numerically as follows.

*Step 0.* Choose an initial body shape  $\Gamma_i (i = 0)$  appropriately and the basis functions  $\rho_k (k = 1, \dots, N)$  of the boundary variation.

*Step 1.* Generate a computational grid in the domain  $\Omega_i$  bounded by  $\Gamma_\varepsilon$  and  $\Gamma_i$ .

*Step 2.* Obtain  $u$ , the solution of the direct problem, and then  $p$ , the solution of the adjoint problem.

*Step 3.* Obtain the first variations  $\phi_k$  and  $\pi_k$  of solutions of the direct and adjoint problems for each  $k$ .

*Step 4.* Determine the modified shape  $\Gamma_\varepsilon$  according to the process described in the previous subsection. Let  $\Gamma_\varepsilon$  be  $\Gamma_{i+1}$ .

*Step 5.* Go to Step 1 unless the change in body shape is smaller than a prescribed convergence parameter.

Glowinski and Pironneau<sup>5</sup> (also Çabuk and Modi<sup>6</sup>) proposed a shape modification procedure based on (9) by displacing  $\Gamma_0$  normally through a distance proportional to  $\Lambda_0 - k$ , where  $k$  is the mean value of  $\Lambda_0$  on  $\Gamma_0$ . Numerical experiments show that the iteration method suggested in Reference 5 permits only very small deformation of the shape to prevent new boundary nodes from coalescing and requires relocation of boundary points to damp small-amplitude wiggles which deteriorate the numerical results in the subsequent calculation.

On the other hand, the shape modification procedure proposed in the present study, at the expense of computing the first variations  $\phi_k$  and  $\pi_k$ , is shown experimentally to permit much larger deformations yet still give an acceptably smooth shape and thus many fewer iterations are needed for convergence to the optimal shape. Moreover, for the numerical calculation of the first variations of 16 pairs of  $\phi_k$  and  $\pi_k$  at  $Re = 20$  the required CPU time was about the same as that for  $u$  and  $p$ .

In the actual experiment we have chosen the scale  $\varepsilon_0$  moderately large at first and employed a small number of basis functions ( $N \leq 3$  or 4). If the optimal boundary variation lies in the interior of inequality constraint (21), we choose a new  $\varepsilon_0$  smaller than the previous one and increase the number



of basis functions. The second-order necessary condition (14) was satisfied for each optimal shape obtained.

Since the optimal shape is assumed to be symmetric with respect to the  $x$ -axis (the direction of outer flow), we expand  $\rho$  in a Fourier cosine series, taking into consideration constraint (11):

$$\rho = \sum_{k=1}^N a_k \cos\left(\frac{k\pi s}{L}\right), \quad (22)$$

where  $s$  denotes the arc length parameter of  $\Gamma_i$  measured from the rear end and  $L$  denotes the half-length of profile  $\Gamma_i$ .

Local analysis near the ends of the two-dimensional optimal body<sup>4</sup> shows that the ends of the body must each be tangential to a wedge of angle  $102.6^\circ$ . Since the basic profile modification method (Step 4) with the boundary variation given by (22) can give only a smooth profile, we revise Step 4 in order to admit wedge shapes near the ends as follows.

*Step 4'*. From the profile obtained by the basic profile modification method, calculate the tangents at the nodes next nearest to the front and rear ends (second nodes from the ends) and determine new end-points as the intersection points of the tangents and the  $x$ -axis. To join the end regions smoothly with the remaining part, construct splines using the end nodes and the second and third nodes from each end. In addition, assign the midpoint as the nearest node to each end on the spline. Since the profile obtained by the above procedure may change the area of the profile, scale the whole profile to yield the given area.

### 4.3. Numerical results

Numerical calculations are carried out using the finite difference method. The computational grid is generated by finding the conformal mapping of the unbounded flow region into a rectangle using the method suggested by Moretti.<sup>11</sup> The grid is regenerated for various shapes which are formed during the iterative optimization process. A typical grid is shown in Figure 2. It is a perfectly orthogonal grid system from conformality.

Since we are interested in the minimum drag profile in a uniform flow in an unbounded region, the computational domain should be sufficiently large that the final results are not affected significantly by a change in domain size. After several numerical experiments the location of the far boundary was chosen at a distance of about 25 times the chord length of the body. Any further increase in domain size caused a change in drage of less than 0.5% at  $Re = 20$  with a  $90 \times 96$  grid. The effect of grid size on the optimal shape is difficult to determine, since the optimal profile is not known *a priori*. Using grids of  $45 \times 48$ ,  $70 \times 96$ ,  $90 \times 96$  and  $90 \times 128$ , calculations of the optimal shape at  $Re = 20$  were carried out. The results show that the difference between optimal shapes for the last three grids is negligibly small and that the drag agrees within 0.1% error. We have chosen a grid size of  $90 \times 96$  for the results presented in this work.

All numerical solutions of the Navier–Stokes equations, the adjoint problem and the first-variation problem are obtained by successive overrelaxation (SOR) after formulating the problems as coupled second-order equations. This streamfunction–vorticity-like formulation adopted in the present study is superior to others in that the proposed optimization algorithm needs only the second derivatives of solutions. Çabuk and Modi<sup>6</sup> have reported difficulties in solving the adjoint problem in a plane diffuser. In our case of external flow a coarse grid in the far field can cause instability in the solution of the adjoint problem. To overcome this difficulty, a fine mesh has been adopted in the far field as shown in Figure 2.

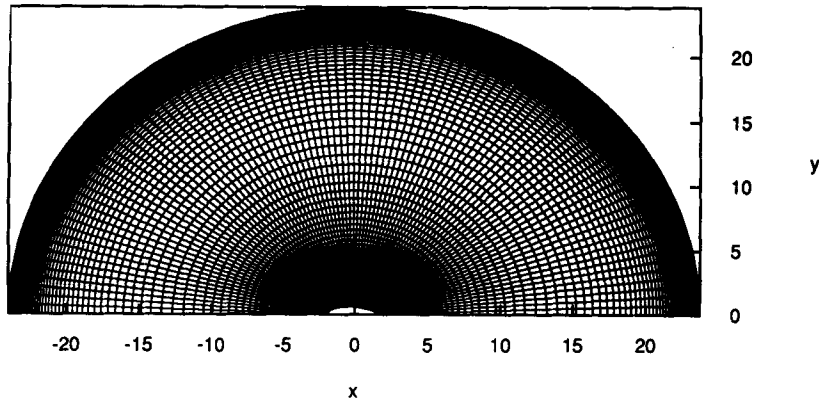


Figure 2. Typical grid ( $90 \times 60$ ) generated using conformal mapping

Using the algorithm described above, two-dimensional optimal shapes are obtained for a body of area  $\pi$  at Reynolds numbers  $Re = 1, 10, 20$  and  $40$ . The calculation at  $Re = 20$  (the reference case) has been examined in particular detail to discuss convergence and accuracy.

Since the present algorithm relies on the prediction of solutions of the direct and adjoint problems for the deformed body, it is essential to test the accuracy of approximate solutions obtained on the basis of first variations. Therefore a test case where the boundary variation  $\varepsilon\rho = \varepsilon \cos(2s)$  is given on the unit circle is calculated at  $Re = 20$ . Figure 3 compares the exact distributions of  $\partial^2 u / \partial n^2$  and  $\partial^2 p / \partial n^2$  on the perturbed body and those obtained from the prediction method for  $\varepsilon = 0.1$  and  $0.05$ . As seen in the figure, the predicted and numerical (exact) results for the perturbed body are indistinguishable for  $\varepsilon = 0.05$ .

Figure 4 illustrates the optimal shape as well as the profiles at successive iterations starting from the unit circle at  $Re = 20$ . As seen in the figure, the angle of the wedge-shaped front and rear end regions approaches  $102.6^\circ$  as expected by the local analysis. In Figure 5 the distribution of  $\Lambda_\varepsilon$  (which should be constant on the optimal profile) on the profile at each intermediate iteration is depicted. The constancy of  $\Lambda_\varepsilon$  on the final profile is satisfied fairly well except near the front end of the body.

In Figure 6 the distributions of pressure and skin friction for a circular cylinder and the numerically obtained optimal shape are illustrated. A rapid decrease in pressure seems to result in a decrease in the

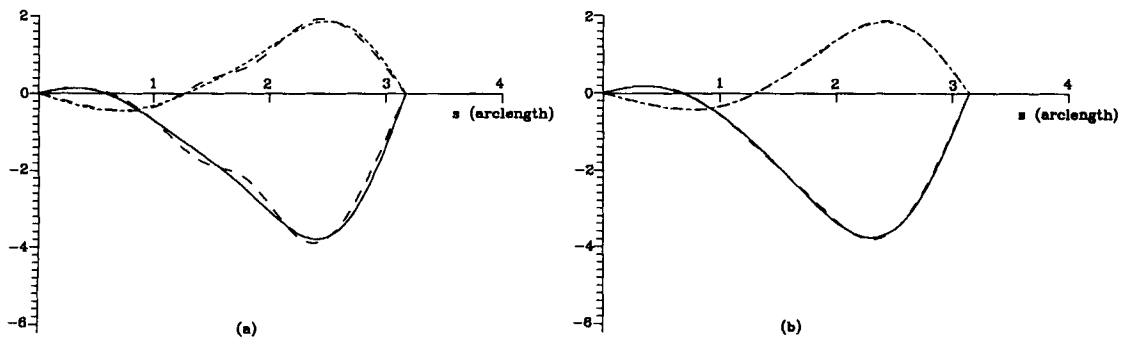


Figure 3. Comparison of exact and approximate distributions of  $\partial^2 u / \partial n^2$  (vorticity) and  $\partial^2 p / \partial n^2$  (adjoint vorticity) on perturbed surface ( $\rho = \cos(2s)$ ) for (a)  $\varepsilon = 0.1$  and (b)  $\varepsilon = 0.05$ . The full curve represents the numerically obtained exact distribution of  $\partial^2 u / \partial n^2$  and the dotted curve the exact distribution of  $\partial^2 p / \partial n^2$ . Broken curves represent approximate distributions obtained by first-order variations

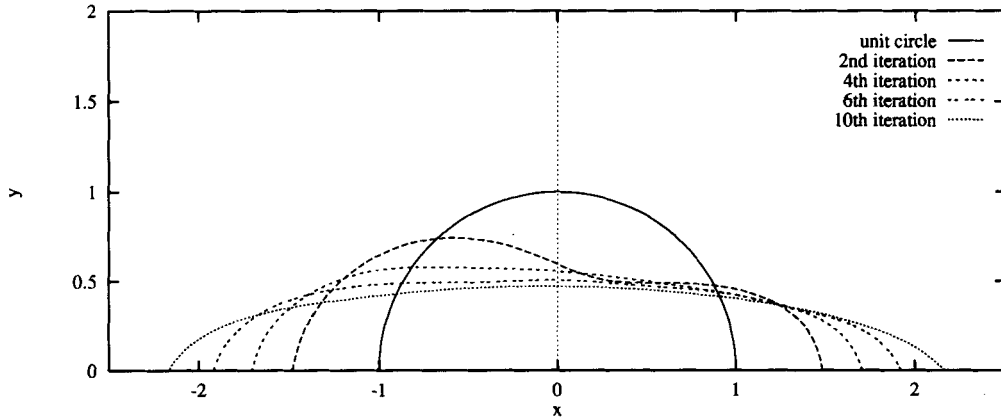


Figure 4. Profiles ( $Re = 20$ ) at successive iterations

drag force exerted on the body. As seen in the figure, the pressure decreases rapidly near the front end and then becomes nearly constant. The total drag on the body is comprised of the friction drag due to the tangential stress at the body surface and the form drag due to the normal stress. In Table I the values of friction drag, form drag and total drag at successive iterations are listed. The successive iteration of the profile modification process results in a more rapid decrease in the form drag than increase in the

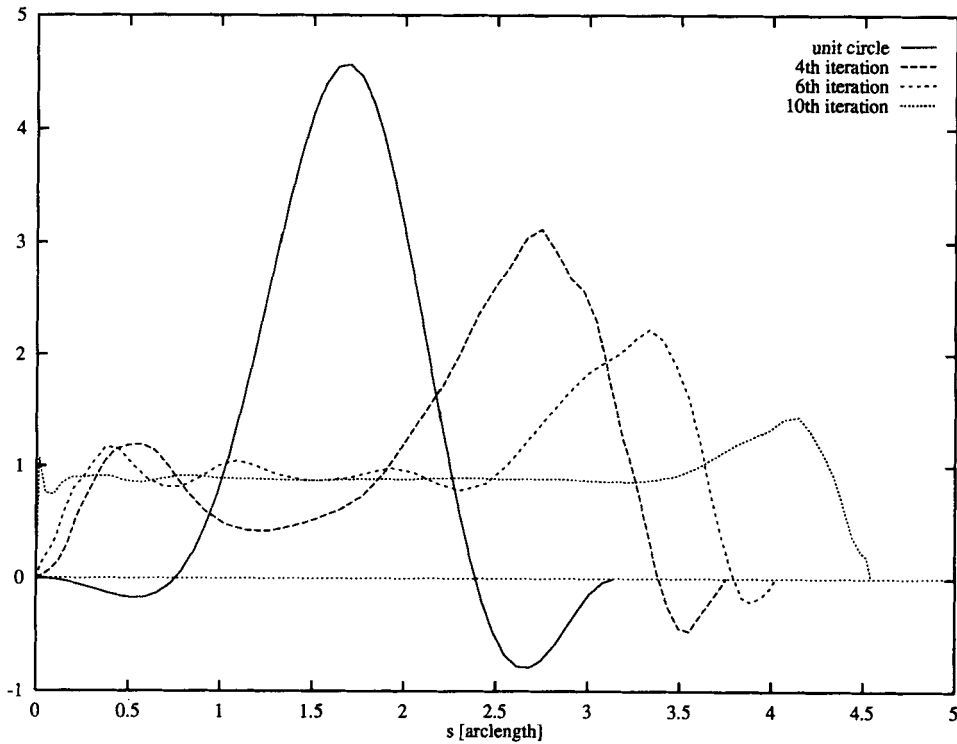


Figure 5. Distributions of  $\Lambda_e$  at successive iterations ( $Re = 20$ ). At the 10th iteration  $\Lambda_e$  becomes almost constant except near the front and rear ends

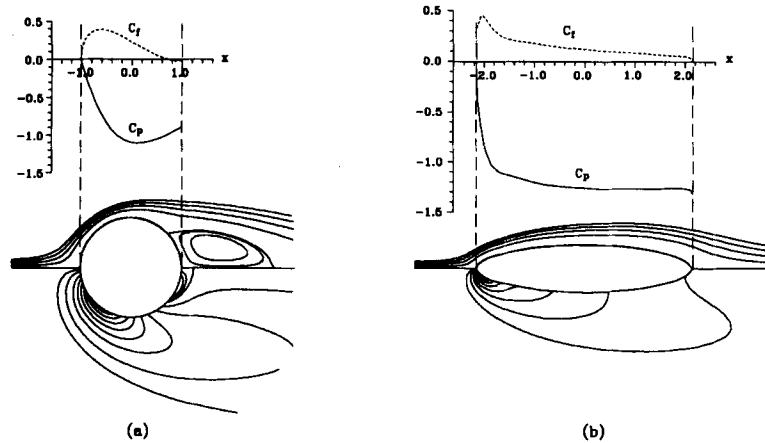


Figure 6. Distributions of pressure and skin friction on (a) circular cylinder and (b) optimal profile ( $Re = 20$ ). Streamlines (upper part) and equivorticity lines (lower part) are also depicted

friction drag and thus in a reduction of the total drag. For the calculations at other Reynolds numbers in the present study the same tendency is observed (Table II).

If the optimal shape is unique for steady flow at a given Reynolds number, the algorithm should give the same final result independently of the initial choice of body shape. The optimal shape determined iteratively from the unit circle and that from the optimal ellipse of smallest drag (major axis/minor axis = 2.11/0.47) are almost identical. The optimal ellipses at  $Re = 1, 10$  and 40 have major axis/minor axis ratios of 1.56/0.64, 1.94/0.51 and 2.29/0.44 respectively. Figure 7 shows the minimum drag profiles determined from the optimal ellipses at  $Re = 1, 10, 20$  and 40. The optimal shape becomes longer and thinner at higher Reynolds number. The overall profile is found to be very close to the optimal ellipse and about one or two iterations were sufficient to find the optimal shape at a given Reynolds number.

Since it is known that the flow at high Reynolds number is in general unsteady, we have not considered the optimal shapes for high-Reynolds-number cases. However, if a steady flow exists, the proposed algorithm is expected to work well.

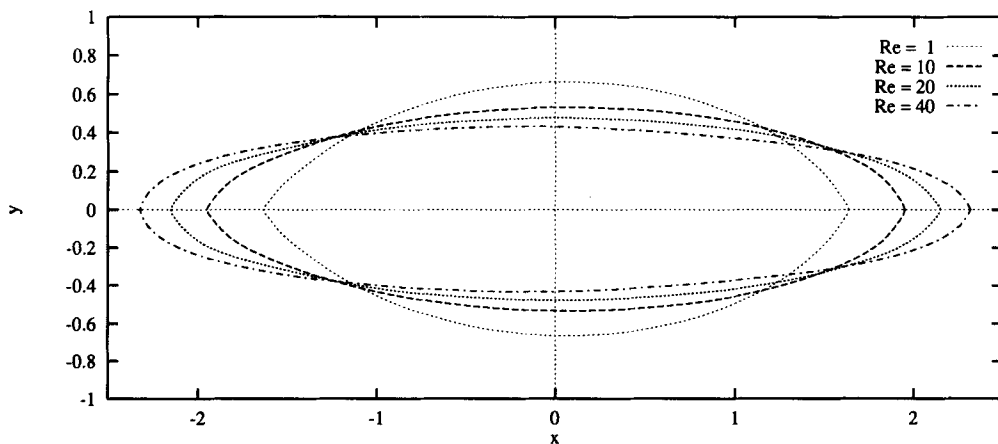


Figure 7. Optimal profiles at various Reynolds numbers

Table I. Values of friction drag, form drag and total drag at successive iterations ( $Re = 20$ )

Iteration	Form drag	Friction drag	Total drag
0	1.182	0.785	1.967
2	0.839	0.892	1.730
4	0.616	1.038	1.654
6	0.495	1.132	1.628
8	0.403	1.216	1.619
10	0.363	1.254	1.617

Table II. Comparison of friction drag, form drag and total drag for circular cylinder, optimal ellipse and optimal body (area  $\pi$ ) at various Reynolds numbers

$Re$	Circular cylinder			Optimal ellipse			Optimal profile		
	Form drag	Friction drag	Total drag	Form drag	Friction drag	Total drag	Form drag	Friction drag	Total drag
1	5.219	5.107	10.325	2.924	6.962	9.886	2.628	7.249	9.877
10	1.525	1.195	2.720	0.583	1.790	2.373	0.573	1.800	2.373
20	1.182	0.785	1.967	0.379	1.235	1.614	0.355	1.259	1.614
40	0.954	0.508	1.462	0.252	0.859	1.112	0.252	0.859	1.111

5. CONCLUSIONS

A shape optimization problem in two-dimensional steady viscous flow is considered. The first- and second-order necessary optimality conditions are derived in terms of a streamfunction which satisfies a fourth-order partial differential equation with the biharmonic operator as principal part. Thus the present approach may be considered as a direct generalization of that of Fujii,<sup>8-10</sup> who considered a second-order partial differential equation with the Laplacian operator as principal part. The first-order optimality condition is equivalent to that derived by Pironneau.<sup>3</sup>

To determine the optimal shape numerically, an algorithm is proposed in which the first variations of solutions of the direct and adjoint problems are incorporated. Numerical experiments carried out for low Reynolds numbers ( $Re \leq 40$ ) show that the present algorithm gives satisfactory results after a few iterations.

APPENDIX I: PROOF OF A CHARACTERIZATION THEOREM

Let  $Q(\mathbf{x}, \xi)$  and  $K(\mathbf{x}, \xi)$  be fundamental solutions of the biharmonic operator  $-\Delta^2$  and the harmonic operator  $-\Delta$  having singularity at  $\xi$  respectively. We choose

$$Q(\mathbf{x}, \xi) = \frac{1}{8\pi} |\mathbf{x} - \xi|^2 \left[ \log \left( \frac{1}{|\mathbf{x} - \xi|} \right) + 1 \right],$$

$$K(\mathbf{x}, \xi) = \frac{1}{2\pi} \log \left( \frac{1}{|\mathbf{x} - \xi|} \right).$$

Note that  $\Delta_{\mathbf{x}} Q(\mathbf{x}, \xi) = K(\mathbf{x}, \xi)$ .

For any  $\xi \in \Omega \cup \bar{\Omega}^c$  let us introduce two boundary integrals defined on the boundary  $\Gamma$  of a domain  $\Omega$  in  $\mathbb{R}^2$ :

$$F_v^\Gamma(\xi) = \int_\Gamma \left( K(\mathbf{x}, \xi) \frac{\partial v}{\partial n}(\mathbf{x}) - v(\mathbf{x}) \frac{\partial K}{\partial n}(\mathbf{x}, \xi) \right) d\Gamma,$$

$$S_v^\Gamma(\xi) = \int_\Gamma \left( Q(\mathbf{x}, \xi) \frac{\partial(\Delta v)}{\partial n}(\mathbf{x}) - \Delta v(\mathbf{x}) \frac{\partial Q}{\partial n}(\mathbf{x}, \xi) \right) d\Gamma,$$

where  $d\Gamma$  is the length element of  $\Gamma$ . Then for any  $\xi \in \Omega \cup \bar{\Omega}^c$  and  $v \in C^4(\bar{\Omega})$  it is known<sup>12</sup> that

$$p(\xi) \cdot v(\xi) = - \int_\Omega Q(\mathbf{x}, \xi) \Delta^2 v(\mathbf{x}) d\Omega + F_v^\Gamma(\xi) + S_v^\Gamma(\xi),$$

where the function  $p(\xi)$  on  $\Omega \cup \bar{\Omega}^c$  is defined by  $p(\xi) = 1$  if  $\xi \in \Omega$  or  $p(\xi) = 0$  if  $\xi \in \bar{\Omega}^c$ . Then we claim the following lemma.

*Lemma*

Suppose a function  $v(\xi) \in C^4(\bar{\Omega})$  satisfies an integral equation such that for any  $\xi \in \Omega \cup \bar{\Omega}^c$ ,

$$p(\xi) \cdot v(\xi) = - \int_\Omega Q(\mathbf{x}, \xi) \Delta^2 v(\mathbf{x}) d\Omega + S_v^\Gamma(\xi) + \int_\Gamma \left( K(\mathbf{x}, \xi) v(\mathbf{x}) - \frac{\partial K(\mathbf{x}, \xi)}{\partial n} \mu(\mathbf{x}) \right) d\Gamma,$$

where  $v(\mathbf{x})$  and  $\mu(\mathbf{x})$  are continuously differentiable functions defined on  $\Gamma$ . Then  $v|_\Gamma = \mu$  and  $\partial v / \partial n|_\Gamma = v$ .

*Proof.* Let  $u(\xi) \in C^4(\bar{\Omega})$  be a function with boundary values  $u|_\Gamma = \mu$  and  $\partial u / \partial n|_\Gamma = v$ . Then for any  $\xi \in \Omega \cup \bar{\Omega}^c$ ,  $u$  satisfies

$$p(\xi) \cdot u(\xi) = - \int_\Omega Q(\mathbf{x}, \xi) \Delta^2 u(\mathbf{x}) d\Omega + F_u^\Gamma(\xi) + S_u^\Gamma(\xi).$$

Putting  $w(\xi) = u(\xi) - v(\xi)$ , then obviously  $w(\xi) \in C^4(\bar{\Omega})$  and we have

$$\begin{aligned} p(\xi) \cdot w(\xi) &= - \int_\Omega Q(\mathbf{x}, \xi) \Delta^2 w(\mathbf{x}) d\Omega + S_w^\Gamma(\xi) \\ &= - \int_\Omega K(\mathbf{x}, \xi) \Delta w(\mathbf{x}) d\Omega. \end{aligned} \quad (23)$$

The last equality is obtained by integration by parts. After applying the following integral identity for the Laplacian operator to (23)

$$\int_\Omega K(\mathbf{x}, \xi) \Delta w(\mathbf{x}) d\Omega = -p(\xi) \cdot w(\xi) + F_w^\Gamma(\xi),$$

we have  $F_w^\Gamma(\xi) = 0$  or

$$\int_\Gamma w(\mathbf{x}) \frac{\partial K(\mathbf{x}, \xi)}{\partial n} d\Gamma = \int_\Gamma K(\mathbf{x}, \xi) \frac{\partial w(\mathbf{x})}{\partial n} d\Gamma. \quad (24)$$

The left-hand side of (24) (denoted by  $D(\xi)$ ) is the potential of a double layer with density distribution  $w(\mathbf{x})$  on  $\Gamma$ , while the right-hand side (denoted by  $S(\xi)$ ) is that of a single layer with density distribution  $(\partial w / \partial n)(\mathbf{x})$  on  $\Gamma$ . Let  $\xi_0$  be an arbitrary point on  $\Gamma$ . By the jump discontinuity property of

the potential of a double layer, as  $\xi$  approaches  $\xi_0$  from the inside of  $\Gamma$ ,

$$D(\xi_0) - \frac{1}{2}w(\xi_0) = S(\xi_0), \quad (25)$$

and as  $\xi$  goes to  $\xi_0$  from the outside of  $\Gamma$ ,

$$D(\xi_0) + \frac{1}{2}w(\xi_0) = S(\xi_0), \quad (26)$$

since the potential of a single layer is continuous up to the boundary.<sup>12</sup> Therefore we conclude that  $w(\xi) = 0$  for all  $\xi \in \Gamma$  from (25) and (26), since  $\xi_0$  is an arbitrary point on  $\Gamma$ .

Finally, since the single-layer potential  $S(\xi)$  is identically zero in  $\Omega \cup \bar{\Omega}^c$ ,

$$0 = \lim_{\substack{\xi \rightarrow \xi_0 \\ \xi \in L_{\xi_0} \cap \bar{\Omega}^c}} \frac{\partial S}{\partial n_\xi}(\xi) = \lim_{\substack{\xi \rightarrow \xi_0 \\ \xi \in L_{\xi_0} \cap \Omega}} \frac{\partial S}{\partial n_\xi}(\xi) = -\frac{\partial w}{\partial n}(\xi_0),$$

where  $L_{\xi_0}$  is the line through  $\xi_0$  along the outward normal to  $\Gamma$  at  $\xi_0 \in \Gamma$ . We have proved the assertion.  $\square$

Using the lemma, we show that the variations  $\phi$  and  $\psi$  are characterized as the solutions of boundary value problems similar to (1).

*Theorem.*

Under assumptions A1 and A2 of Section 3 the first variation of the solution satisfies the boundary value problem

$$Re^{-1}\Delta^2\phi = \frac{\partial(\delta u, \phi)}{\partial(x, y)} + \frac{\partial(\Delta\phi, u)}{\partial(x, y)} \quad \text{in } \Omega,$$

$$\phi|_{\Gamma^b} = 0, \quad \frac{\partial\phi}{\partial n}\Big|_{\Gamma^b} = -\rho \frac{\partial^2 u}{\partial n^2}, \quad \phi|_{\Gamma^c} = \frac{\partial\phi}{\partial n}\Big|_{\Gamma^c} = 0$$

and the second variation of the solution also satisfies the fourth-order elliptic boundary value problem

$$Re^{-1}\Delta^2\psi = \frac{\partial(\Delta\phi, \phi)}{\partial(x, y)} + \frac{\partial(\Delta u, \psi)}{\partial(x, y)} + \frac{\partial(\Delta\psi, u)}{\partial(x, y)} \quad \text{in } \Omega,$$

$$\psi|_{\Gamma^b} = -\frac{1}{2}\rho \frac{\partial\phi}{\partial n}, \quad \frac{\partial\psi}{\partial n}\Big|_{\Gamma^b} = \frac{1}{2}\kappa\rho^2 \frac{\partial^2 u}{\partial n^2} - \sigma \frac{\partial^2 u}{\partial n^2} - \frac{1}{2}\rho^2 \frac{\partial(\Delta u)}{\partial n} - \rho \frac{\partial^2\phi}{\partial n^2}, \quad \psi|_{\Gamma^c} = \frac{\partial\psi}{\partial n}\Big|_{\Gamma^c} = 0.$$

Here  $\kappa$  is the curvature of  $\Gamma$ .

*Proof.* For the sake of simplicity we give the proof for the case where  $\Omega \subset \Omega_e$ . For the general case where  $\Omega \not\subset \Omega_e$  the same conclusion can be obtained with slight modifications. The integral expressions for  $u(\xi) \in C^4(\bar{\Omega})$  and  $u_e(\xi) \in C^4(\Omega_e)$ , the solutions of the partial differential equations (1) in domains  $\Omega$  and  $\Omega_e$ , respectively, are formally given by

$$u(\xi) = -Re \int_{\Omega} Q(\mathbf{x}, \xi) \frac{\partial(\Delta u, u)}{\partial(x, y)} d\Omega + F_u^\Gamma(\xi) + S_u^\Gamma(\xi) \quad (27)$$

and

$$u_e(\xi) = -Re \int_{\Omega_e} Q(\mathbf{x}, \xi) \frac{\partial(\Delta u_e, u_e)}{\partial(x, y)} d\Omega + F_{u_e}^{\Gamma_e}(\xi) + S_{u_e}^{\Gamma_e}(\xi) \quad (28)$$

for any  $\xi \in \Omega$

Subtracting (27) from (28), we have

$$\begin{aligned}
u_\varepsilon(\xi) - u(\xi) &= -Re \left( \int_{\Omega_\varepsilon} Q(\mathbf{x}, \xi) \frac{\partial(\Delta u_\varepsilon, u_\varepsilon)}{\partial(x, y)} d\Omega - \int_{\Omega} Q(\mathbf{x}, \xi) \frac{\partial(\Delta u, u)}{\partial(x, y)} d\Omega \right) \\
&\quad + [F_{u_\varepsilon}^{\Gamma_\varepsilon}(\xi) - F_u^\Gamma(\xi)] + [S_{u_\varepsilon}^{\Gamma_\varepsilon}(\xi) - S_u^\Gamma(\xi)] \\
&\equiv I_1^\varepsilon + I_2^\varepsilon + I_3^\varepsilon.
\end{aligned} \tag{29}$$

The second integral  $I_2^\varepsilon$  vanishes, since  $u_\varepsilon$  and  $u$  satisfy the same boundary conditions on  $\Gamma_\varepsilon$  and  $\Gamma$  respectively. Since  $\Omega \subset \Omega_\varepsilon$ , the first integral can be written as

$$\begin{aligned}
I_1^\varepsilon &= -Re \left[ \int_{\Omega_\varepsilon - \Omega} Q(\mathbf{x}, \xi) \frac{\partial(\Delta u_\varepsilon, u_\varepsilon)}{\partial(x, y)} d\Omega + \int_{\Omega} Q(\mathbf{x}, \xi) \left( \frac{\partial(\Delta u_\varepsilon, u_\varepsilon)}{\partial(x, y)} - \frac{\partial(\Delta u, u)}{\partial(x, y)} \right) d\Omega \right] \\
&= - \int_{\Omega_\varepsilon - \Omega} Q(\mathbf{x}, \xi) \frac{\partial(\Delta u_\varepsilon, u_\varepsilon)}{\partial(x, y)} d\Omega - \varepsilon \int_{\Omega} Q(\mathbf{x}, \xi) \left( \frac{\partial(\Delta u, \phi)}{\partial(x, y)} + \frac{\partial(\Delta \phi, u)}{\partial(x, y)} \right) d\Omega \\
&\quad - \varepsilon^2 \int_{\Omega} Q(\mathbf{x}, \xi) \left( \frac{\partial(\Delta \phi, \phi)}{\partial(x, y)} + \frac{\partial(\Delta u, \psi)}{\partial(x, y)} + \frac{\partial(\Delta \psi, u)}{\partial(x, y)} \right) d\Omega + O(\varepsilon^3).
\end{aligned} \tag{30}$$

Using Green's identities and the fact that  $u_\varepsilon - u = \varepsilon\phi + \varepsilon^2\psi + O(\varepsilon^3)$ , we have

$$\begin{aligned}
I_3^\varepsilon &= \left( \int_{\Omega_\varepsilon - \Omega} Q(\mathbf{x}, \xi) \Delta^2 u_\varepsilon(\mathbf{x}) d\Omega - \int_{\Omega_\varepsilon - \Omega} \Delta_{\mathbf{x}} Q(\mathbf{x}, \xi) \Delta u_\varepsilon(\mathbf{x}) d\Omega \right) \\
&\quad + \left[ \int_{\Gamma} Q(\mathbf{x}, \xi) \left( \varepsilon \frac{\partial \Delta \phi}{\partial n}(\mathbf{x}) + \varepsilon^2 \frac{\partial \Delta \psi}{\partial n}(\mathbf{x}) \right) d\Gamma \right. \\
&\quad \left. - \int_{\Gamma} [\varepsilon \Delta \phi(\mathbf{x}) + \varepsilon^2 \Delta \psi(\mathbf{x})] \frac{\partial Q}{\partial n}(\mathbf{x}, \xi) d\Gamma \right] + O(\varepsilon^3).
\end{aligned}$$

The second term in large parentheses can be written as a sum of line integrals along  $\Gamma$  using the following formula given in Reference 9 for  $w(\mathbf{x}) \in C^2(\overline{\Omega_\varepsilon} - \overline{\Omega})$ :

$$\begin{aligned}
\int_{\Omega_\varepsilon - \Omega} w(\mathbf{x}) d\Omega &= \varepsilon \int_{\Gamma} w(\mathbf{x}) \rho(\mathbf{x}) d\Gamma + \varepsilon^2 \int_{\Gamma} w(\mathbf{x}) \sigma(\mathbf{x}) d\Gamma \\
&\quad + \frac{1}{2} \varepsilon^2 \int_{\Gamma} \left( \frac{\partial w}{\partial n}(\mathbf{x}) + \kappa w(\mathbf{x}) \right) \rho^2(\mathbf{x}) d\Gamma + O(\varepsilon^3),
\end{aligned}$$

where  $\kappa$  is the curvature of  $\Gamma$  is defined as positive when the curve  $\Gamma$  is convex to the domain. Rearranging  $I_3^\varepsilon$  in powers of  $\varepsilon$ , we have

$$\begin{aligned}
I_3^\varepsilon &= \int_{\Omega_\varepsilon - \Omega} Q(\mathbf{x}, \xi) Re \frac{\partial(\Delta u_\varepsilon, u_\varepsilon)}{\partial(x, y)} d\Omega - \left[ \varepsilon \int_{\Gamma^b} [K(\mathbf{x}, \xi) \Delta u(\mathbf{x})] \rho(\mathbf{x}) d\Gamma \right. \\
&\quad + \varepsilon^2 \left( \int_{\Gamma^b} [K(\mathbf{x}, \xi) \Delta \phi(\mathbf{x})] \rho(\mathbf{x}) d\Gamma + \int_{\Gamma^b} [K(\mathbf{x}, \xi) \Delta u(\mathbf{x})] \sigma(\mathbf{x}) d\Gamma \right) \\
&\quad + \frac{1}{2} \varepsilon^2 \int_{\Gamma^b} \left( \frac{\partial(K \Delta u)}{\partial n}(\mathbf{x}, \xi) + \kappa [K(\mathbf{x}, \xi) \Delta u(\mathbf{x})] \right) \rho^2(\mathbf{x}) d\Gamma \left. \right] \\
&\quad + \varepsilon S_\phi^\Gamma(\xi) + \varepsilon^2 S_\psi^\Gamma(\xi) + O(\varepsilon^3).
\end{aligned} \tag{31}$$



Substitution of (30) and (31) into (29) gives

$$\begin{aligned}
 u_\varepsilon(\xi) - u(\xi) = & - \left[ \varepsilon \int_{\Omega} Q(\mathbf{x}, \xi) Re \left( \frac{\partial(\Delta u, \phi)}{\partial(x, y)} + \frac{\partial(\Delta \phi, u)}{\partial(x, y)} \right) d\Omega \right. \\
 & + \varepsilon^2 \int_{\Omega} Q(\mathbf{x}, \xi) Re \left( \frac{\partial(\Delta \phi, \phi)}{\partial(x, y)} + \frac{\partial(\Delta u, \psi)}{\partial(x, y)} + \frac{\partial(\Delta \psi, u)}{\partial(x, y)} \right) d\Omega \Big] \\
 & + \varepsilon \left( S_{\phi}^{\Gamma}(\xi) - \int_{\Gamma^b} K(\mathbf{x}, \xi) \Delta u(\mathbf{x}) \rho(\mathbf{x}) d\Gamma \right) \\
 & + \varepsilon^2 \left[ S_{\psi}^{\Gamma}(\xi) - \int_{\Gamma^b} K(\mathbf{x}, \xi) \Delta \phi(\mathbf{x}) \rho(\mathbf{x}) d\Gamma \right. \\
 & - \int_{\Gamma^b} K(\mathbf{x}, \xi) \Delta u(\mathbf{x}) \sigma(\mathbf{x}) d\Gamma \\
 & \left. - \int_{\Gamma} \frac{1}{2} \left( \frac{\partial(K \Delta u)}{\partial n}(\mathbf{x}, \xi) + \kappa K(\mathbf{x}, \xi) \Delta u(\mathbf{x}) \right) \rho^2(\mathbf{x}) d\Gamma \right] + O(\varepsilon^3).
 \end{aligned}$$

Since the left-hand side is expressed as  $\varepsilon \phi(\xi) + \varepsilon^2 \psi(\xi) + O(\varepsilon^3)$  for sufficiently small  $\varepsilon$ , equating like powers of  $\varepsilon$  on each side, we obtain the integral equation for the first variation  $\phi$

$$\phi(\xi) = - \int_{\Omega} Q(\mathbf{x}, \xi) Re \left( \frac{\partial(\Delta u, \phi)}{\partial(x, y)} + \frac{\partial(\Delta \phi, u)}{\partial(x, y)} \right) d\Omega + \int_{\Gamma^b} K(\mathbf{x}, \xi) [-\Delta u(\mathbf{x})] \rho(\mathbf{x}) d\Gamma + S_{\phi}^{\Gamma}(\xi), \quad (32)$$

and that for the second variation  $\psi$ ,

$$\begin{aligned}
 \psi(\xi) = & - \int_{\Omega} Q(\mathbf{x}, \xi) Re \left( \frac{\partial(\Delta \phi, \phi)}{\partial(x, y)} + \frac{\partial(\Delta u, \psi)}{\partial(x, y)} + \frac{\partial(\Delta \psi, u)}{\partial(x, y)} \right) d\Omega \\
 & + \left( \int_{\Gamma^b} K(\mathbf{x}, \xi) [-\rho(\mathbf{x}) \Delta \phi(\mathbf{x}) - \sigma(\mathbf{x}) \Delta u(\mathbf{x}) - \frac{1}{2} \kappa \rho^2(\mathbf{x}) \Delta u(\mathbf{x})] d\Gamma \right. \\
 & \left. - \int_{\Gamma^b} \frac{1}{2} \rho^2(\mathbf{x}) \frac{\partial(K \Delta u)}{\partial n}(\mathbf{x}, \xi) d\Gamma \right) + S_{\psi}^{\Gamma}(\xi). \quad (33)
 \end{aligned}$$

From the definitions of the first variation  $\phi$  and the second variation  $\psi$  we observe that they satisfy the following equations under assumptions A1 and A2:

$$\begin{aligned}
 Re^{-1} \Delta^2 \phi &= \frac{\partial(\Delta u, \phi)}{\partial(x, y)} + \frac{\partial(\Delta \phi, u)}{\partial(x, y)} \quad \text{in } \Omega, \\
 Re^{-1} \Delta^2 \psi &+ \frac{\partial(\Delta \phi, \phi)}{\partial(x, y)} + \frac{\partial(\Delta u, \psi)}{\partial(x, y)} + \frac{\partial(\Delta \psi, u)}{\partial(x, y)} \quad \text{in } \Omega.
 \end{aligned} \quad (34)$$

Substituting (34) into (32) and (33) and taking into consideration the lemma, we can see that the boundary values of the first variation of the solution are given by

$$\phi|_{\Gamma^b} = 0, \quad \phi|_{\Gamma^c} = 0, \quad \frac{\partial \phi}{\partial n} \Big|_{\Gamma} = -\rho \Delta u \quad (35a)$$

and those of the second variaton of the solution by

$$\psi|_{\Gamma^b} = \frac{1}{2} \rho^2 \Delta u, \quad \psi|_{\Gamma^c} = 0, \quad \frac{\partial \psi}{\partial n} \Big|_{\Gamma} = -\rho \Delta \phi - \sigma \Delta u - \frac{1}{2} \kappa \rho^2 \Delta u - \frac{1}{2} \rho^2 \frac{\partial \Delta u}{\partial n}. \quad (35b)$$

Since the Laplacian operator in  $(n, s)$  co-ordinates (Figure 1) is written as

$$\Delta = \frac{\partial^2}{\partial n^2} + \kappa \frac{\partial}{\partial n} + \frac{\partial^2}{\partial s^2},$$

the boundary conditions for  $u$  on  $\Gamma^b$  ( $u = \partial u / \partial n = 0$ ) reduce (35) to the conditions stated in the theorem.

## APPENDIX II: PROOF OF EQUATION (9)

Let us consider the following integral identity derived from integration by parts and  $\partial \mathbf{n} / \partial s = \kappa \mathbf{s}$ :

$$\begin{aligned} & 2 \int_{\Omega} [(u_{yy} - u_{xx})(\phi_{yy} - \phi_{xx}) + 4u_{xy}\phi_{xy}] \, d\Omega \\ &= \int_{\Gamma} \left( G_n^0 \frac{\partial \phi}{\partial n} - G_n^1 \phi - G_s^1 \phi + \kappa G_s^0 \phi \right) \, d\Gamma + \int_{\Omega} 2\phi \Delta^2 u \, d\Omega, \end{aligned} \quad (36)$$

$$G_n^0 \equiv -2(u_{yy} - u_{xx})(n_1^2 - n_2^2) + 8u_{xy}n_1n_2, \quad G_n^1 \equiv -2 \frac{\partial(u_{yy} - u_{xx})}{\partial n} (n_1^2 - n_2^2) + 8 \frac{\partial u_{xy}}{\partial n} n_1n_2.$$

$$G_s^0 \equiv 2G_n^0, \quad G_s^1 \equiv 8 \frac{\partial(u_{yy} - u_{xx})}{\partial s} n_1n_2 + 8 \frac{\partial u_{xy}}{\partial s} (n_1^2 - n_2^2),$$

where  $\mathbf{n} = (n_1, n_2)$  denotes the unit outward normal vector to  $\Gamma$ . Using the no-slip condition, we have on  $\Gamma^b$

$$G_n^0 = 2 \frac{\partial^2 u}{\partial n^2}, \quad G_n^1 = 2 \frac{\partial \Delta u}{\partial n} - 4\kappa \frac{\partial^2 u}{\partial n^2},$$

$$G_s^0 = 4 \frac{\partial^2 u}{\partial n^2}, \quad G_s^1 = 8\kappa \frac{\partial^2 u}{\partial n^2}.$$

If we use the adjoint problem (8), then the second integral of (36) can be written as

$$\int_{\Omega} 2\phi \Delta^2 u \, d\Omega = -2 \int_{\Omega} pL\phi \, d\Omega - 2 \int_{\Gamma} \rho \frac{\partial^2 p}{\partial n^2} \frac{\partial^2 u}{\partial n^2} \, d\Gamma,$$

where  $L$  is the linear partial differential operator defined as

$$L(f) = \Delta^2 f - \operatorname{Re} \left( \frac{\partial(\Delta u, f)}{\partial(x, y)} + \frac{\partial(\Delta f, u)}{\partial(x, y)} \right).$$

Finally, since  $L\phi = 0$ , the first variation  $\delta J^{(1)}$  is given by

$$\begin{aligned} \delta J^{(1)} &= \int_{\Gamma^b} \left[ g\rho + G_0^n \left( -\rho \frac{\partial^2 u}{\partial n^2} \right) - (G_1^n + G_1^s - \kappa G_0^s) \phi - 2\rho \frac{\partial^2 p}{\partial n^2} \frac{\partial^2 u}{\partial n^2} \right] \, d\Gamma \\ &= - \int_{\Gamma^b} \left[ \left( \frac{\partial^2 u}{\partial n^2} \right)^2 + 2 \frac{\partial^2 p}{\partial n^2} \frac{\partial^2 u}{\partial n^2} \right] \rho \, d\Gamma. \end{aligned}$$

We have proved the formula for the first variation. The expression for the second variation  $\delta J^{(2)}$  can be obtained by replacing  $\phi$  with  $\psi$  in the above calculation and using the adjoint problem together with (5b, b'); the details are omitted.

## REFERENCES

1. B. M. Kwak, 'A review on shape optimal design and sensitivity analysis', *J. Struct. Mech. Earthq. Eng.*, **483/I-26**, 159–174 (1994).
2. O. Pironneau, 'On optimum profiles in Stokes flow', *J. Fluid Mech.*, **59**, 117–128 (1973).
3. O. Pironneau, 'On optimum design in fluid mechanics', *J. Fluid Mech.*, **64**, 97–110 (1974).
4. A. A. Mironov, 'On the problem of optimization of the shape of a body in a viscous fluid', *J. Appl. Math. Mech. (PMM)*, **39**, 103–108 (1974).
5. R. Glowinski and O. Pironneau, 'On the computation of the minimum-drag profiles in laminar flow', *J. Fluid Mech.*, **72**, 385–389 (1975).
6. H. Çabuk and V. Modi, 'Optimum plane diffusers in laminar flow', *J. Fluid Mech.*, **237**, 373–393 (1992).
7. H. Van Dyke, *Perturbation Methods in Fluid Mechanics*, Parabolic, Stanford, CA, 1975.
8. N. Fujii, 'Necessary conditions for a domain optimization problem in elliptic boundary value problems', *SIAM J. Control Optim.*, **24**, 346–360 (1986).
9. N. Fujii, 'Second-order necessary conditions in a domain optimization problem', *J. Optim. Theory Appl.*, **65**, 223–244 (1990).
10. N. Fujii, 'Second-order necessary optimality conditions for domain optimization problems of the Neumann type', *J. Optim. Theory Appl.*, **65**, 431–445 (1990).
11. G. Moretti, 'Orthogonal grids around difficult bodies', *ALAA J.*, **30**, 933–938 (1992).
12. R. Courant and D. Hilbert, *Methods of Mathematical Physics*, Vol. 2, Interscience, New York, 1962, pp. 240–261.